



## Parent body of (162173) Ryugu: High porosity, early accretion, small size

Wladimir Neumann<sup>1,2</sup>, Matthias Grott<sup>2</sup>, Mario Trieloff<sup>1</sup>, Ralf Jaumann<sup>3</sup>, Jens Biele<sup>4</sup>, Maximilian Hamm<sup>5</sup>, Ekkehard Kührt<sup>6</sup>, and Naoya Sakatani<sup>7</sup>

<sup>1</sup>Heidelberg University, Institute of Earth Sciences

<sup>2</sup>German Aerospace Center (DLR) Berlin

<sup>3</sup>Free University Berlin

<sup>4</sup>German Aerospace Center (DLR) Cologne

<sup>5</sup>University of Potsdam

<sup>6</sup>China Academy of Space Technology, Beijing

<sup>7</sup>Rikkyo University, Tokyo

**Introduction:** Observations of C-type NEAs and properties of carbonaceous chondrites indicate a high porosity of C-type asteroids. Hayabusa2 demonstrated that Ryugu is a low-density rubble-pile<sup>[1]</sup> dominated by large surface boulders<sup>[2]</sup>. Boulder thermal properties imply a microporosity of  $\square_{\text{boulder}} \approx 28\text{-}55\%$ <sup>[3,4]</sup>, substantially higher than for meteorites and indicative of distinct evolution for Ryugu's parent body from that of water-rich CI/CM chondrites, despite spectral similarities. High microporosity values are consistent with a bulk density of  $1190 \pm 20 \text{ kg m}^{-3}$ <sup>[5]</sup>, a bulk porosity of  $\approx 50\%$ <sup>[1]</sup>, and a macroporosity of  $\approx 16\%$ <sup>[6]</sup>.

We calculated the temperature and porosity evolution for primordial planetesimals and constrained the range of parameters resulting in microporosities compatible with Ryugu's and likely burial depths for the surface boulders. By varying the accretion time  $t_0$  and radius  $R$  and by comparing the porosity distribution with  $\square_{\text{boulder}}$ , hydration, and partial dehydration, we constrained a field within the  $(R, t_0)$ -diagram appropriate for bodies that are likely to have produced such material.

**Methods:** Within the sequence of the parent body evolution, a series of suggested disruption and accretion of intermediate bodies events, and the accretion of Ryugu<sup>[5]</sup>, the boulder microporosity results mainly from parent body processes, e.g., <sup>26</sup>Al-induced internal heating, hydration, compaction, and dehydration prior to the first disruption.

We used global thermal evolution and compaction models<sup>[7]</sup> that predict the microporosity established due to creep processes driven by the joint action of temperature and pressure. No notable creep can be expected in late formed and small objects such as Ryugu or in intermediate objects between the first and last disruption events. Thus, we calculated the interior microporosity of primordial planetesimals with different sizes and accretion times in order to reproduce  $\square_{\text{boulder}}$ .

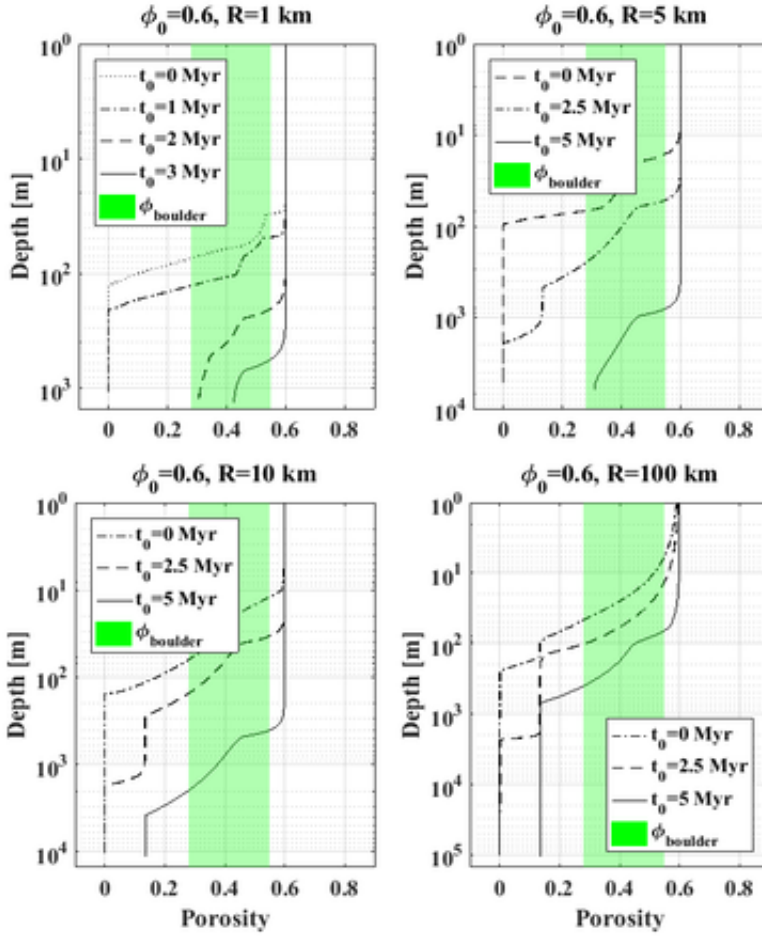


**Fig. 1:** Final porosity profiles for  $R=1, 5, 10,$  and  $100$  km (left to right, top to bottom). Profiles for different accretion times are shown and compared with the  $\phi_{\text{boulder}}$ .

**Results:** The bulk porosity  $\phi_{\text{bulk}}$  calculated shows that large (i.e., slowly cooling and with a higher pressure) and early accreted (i.e.,  $^{26}\text{Al}$ -rich) planetesimals compact more efficiently, retaining only a thin porous blanket. By contrast, low-pressure small and late accreted bodies remain highly porous. While  $\phi_{\text{bulk}}$  provides no information about the porosity distribution, it shows that intermediate conditions with a trade-off between  $R$  and  $t_0$  should result in high volume fractions of material matching  $\phi_{\text{boulder}}$ . Of importance for the accretion of Ryugu from the rubble of a larger object is the location of such material within the parent body. The final porosity distribution is shown in Fig. 1 and compared with  $\phi_{\text{boulder}}$ . Profiles for  $R=1, 5, 10,$  and  $100$  km and several accretion times shown represent different types of structures with up to three layers defined by the comparison  $\phi > \phi_{\text{boulder}}$ ,  $\phi \approx \phi_{\text{boulder}}$ , and  $\phi < \phi_{\text{boulder}}$ .

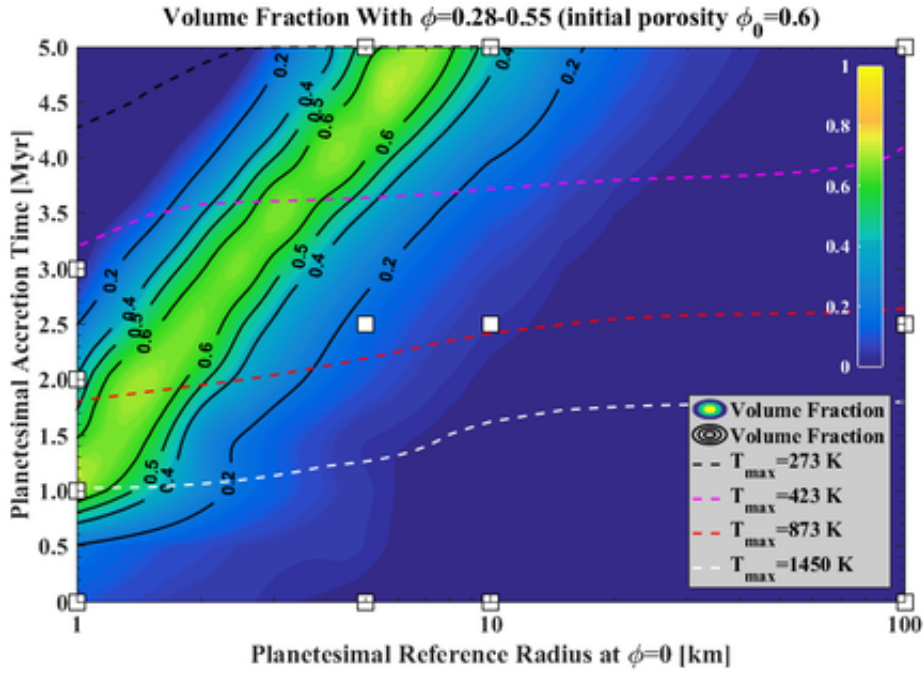


**Fig. 2:** Volume fraction of the material with  $\square \approx \square_{\text{boulder}}$ . Isolines for  $T_{\text{max}}$ : 273 K (onset of aqueous alteration), 873 K (serpentine dehydration), and 1450 K (onset of silicate melting). White squares correspond to bodies from Fig. 1.

A likely parent body needs to have a high fraction  $f_{\text{boulder}}$  of the material with  $\square \approx \square_{\text{boulder}}$ , in particular, if materials from all depths contribute to rubble-piles produced after a disruption<sup>[5]</sup>. Fig. 2 shows that for an initial porosity of  $\square_0 \geq 0.6$ , diagonal maximum fields emerge for  $f_{\text{boulder}}$  confining objects limited by a maximum radius of  $\approx 10$  km and an accretion at 5 Myr after CAIs.

Further observations to be reproduced is aqueous alteration and a partial dehydration. A first-order indicator for hydration (assumed as quasi-instantaneous<sup>[8,9]</sup>) is the water ice melting temperature that is surpassed for a variety of parameter values (Fig. 2, black dashed line), e.g.,  $t_0 \square 4.5$  Myr for km-sized objects (an effect of the rapid decay of <sup>26</sup>Al), and for a late accretion of larger bodies (an effect of their weaker cooling). An upper limit on the thermal conditions is post-dehydration partial melting, occurring for  $1 \square t_0 \square 1.8$  Myr (Fig. 2, white dashed line), that would contradict Ryugu's composition. Thus, only the objects between the black and red lines should have experienced thermal conditions allowing for hydration, and remained cool enough not to dry out.  $T_{\text{max}}$  obtained for a number of models satisfies the CI/CM alteration temperature range, while those between red and white dashed lines indicate dehydration at  $\approx 873$  K, consistent with some carbonaceous chondrites that match Ryugu spectrally<sup>[5,10]</sup>.

Based on the recent detection of boulders with a porosity of 70-90%, additional calculations with an initial porosity of  $\square_0 = 90\%$  that goes beyond the range of 50-80% addressed initially<sup>[7]</sup> were carried out<sup>[11]</sup>. They confirm a parent body size of only a few km (Fig. 3).

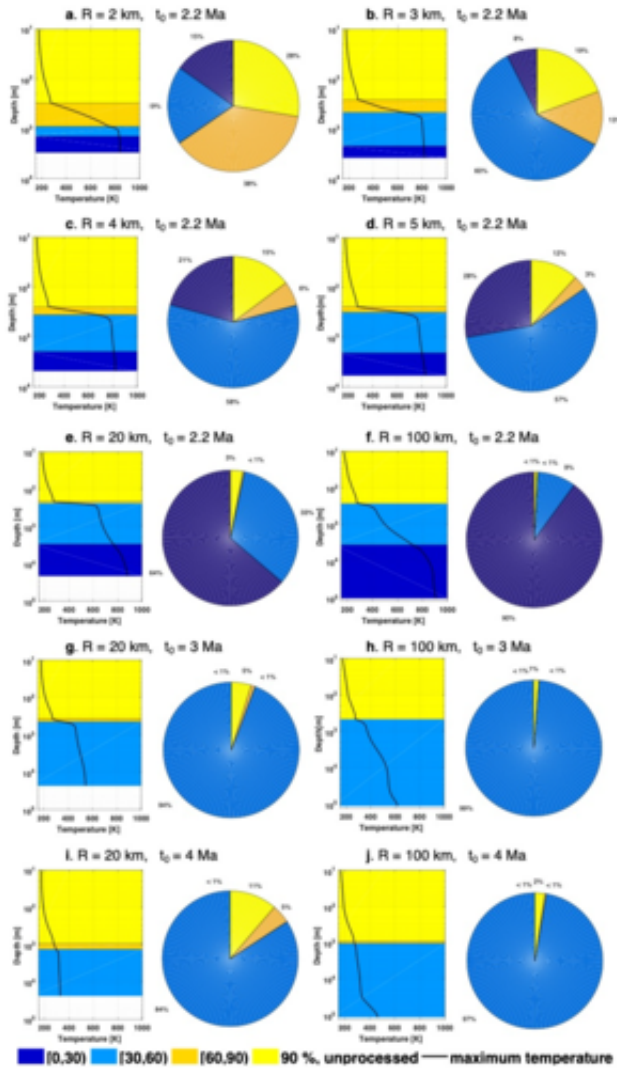


**Fig. 3:** Peak temperature (left panels) and porosity fraction (right panels) for  $\square_0=90\%$ . Porosity distribution for km is most consistent with that of the boulders on Ryugu, i.e., high abundance of boulders with  $30\% < \square_0 < 60\%$  and small fraction of higher and lower porosities.  $T_{\max}$  of the abundant materials is consistent with the estimated dehydration temperature and is homogeneous ( $\approx 800$  K), consistent with the globally uniform spectra on Ryugu.

**Conclusions:** Our calculations indicate a parent body of only a few km that accreted early within  $\square 2$ -3 Myr. Gradual porosity profiles of best-fit bodies indicate production of both low- and high-density boulders from one parent body. By contrast, fits of the carbonate formation data indicate a CI/CM parent body with  $R \approx 20$ -25 km and  $t_0 \approx 3.75$  Myr<sup>[7]</sup>, implying a population of km-sized early accreting highly porous planetesimals as parent bodies of Ryugu and a population of larger and late accreting less porous planetesimals as parent bodies of water-rich chondrites.

**References:** [1] Watanabe S. et al. (2019) *Science*, 364, 268-272. [2] Michikami T. et al. (2019) *Icarus*, 331, 179-191. [3] Grott M. et al. (2019) *NatAst*, 3, 971-976. [4] Hamm M. et al. (2020) *MNRAS*, 496, 2776-2785. [5] Sugita S. et al. (2019) *Science*, 364, eaaw0422. [6] Grott M. et al. (2020) *JGR*, 125, e2020JE006519. [7] Neumann W. et al. (2021) *Icarus*, doi.org/10.1016/j.icarus.2020.114166. [8] Jones C. L. and Brearley A. J. (2006) *GCA*, 70, 1040-1058. [9] Neumann W. et al. (2020) *A&A*, 633, A117. [10] King A. J. et al. (2018) *MAPS*, 54, 521-543. [11] Sakatani N. et al. (2021) *NatAst*, <https://doi.org/10.1038/s41550-021-01371-7>.